INDEPENDENT VIEWS IN MIMO SONAR SYSTEMS

Yan Pailhas[a] & Yvan Petillot[a]

[a]Ocean Systems Lab, Heriot Watt University

Riccarton Campus, EH14 4AS, Scotland, UK
tel: + 44 (0) 131 451 3357, email: Y.Pailhas@hw.ac.uk, www: http://osl.eps.hw.ac.uk/

Abstract: *The main advantages of MIMO (Multiple Input Multiple Output) sonar systems come from the assumption of independent observations between each transmitter/receiver pairs.The independence of the observations ensures a unbiased set of measurements and then provides true statistics on the target. In this paper we study the correlation between views in MIMO sonar systems. A traditional tool used to study the dependency between two random variables is the Pearson product-moment correlation coefficient. However this measure suffers numerous defaults: it only estimates linear correlation, it is not a proper distance and in particular a null measure of the Pearson coefficient does not insure the independence of the tested random variables. For these reasons we will use the distance correlation introduced by Szekely. From the distance correlation we will derive the inter-views distance correlation matrix which assess the correlation of the full MIMO system (i.e. the dependencies between each views). This independence measure matrix gives a guideline to how to build truly uncorrelated MIMO sonar systems and then maximise the performances of such system.*

Keywords: *MIMO sonar systems, Multi-static sonars.*

1. INTRODUCTION

MIMO stands for Multiple Inputs Multiple Outputs. It refers to a structure with spatially spaced transmitters and receivers and has huge implications in wireless communications mainly to overcome the multipath problem in complex urban environments. MIMO sonar systems had raised a lot of interests for ASW purposes. In previous papers [1, 2] we formalised the MIMO theory for wide and narrow band sonar systems. Assuming independent observations between each transmitter/receiver pairs we demonstrated two important results for MIMO systems:

1. it is possible to evaluate the scatterer density of a target if the number of scatterers is low.
2. with a sufficient number of views MIMO systems can decorrelate the scatterers contributions within one pixel resolution and then resolves the speckle.

Result 1. is archived by computing the probability $\mathrm{P}(T_Q|\Gamma)$ as a function of $\mathrm{P}(\Gamma|T_Q)$ using Bayes rules where $\Gamma = \{\gamma_n\}_{n\in[1,N]}$ is the set of observations and T_Q the event of observing a target T with Q scatterers. Assuming the independence of the observations allows us to write:

$$\mathrm{P}(\Gamma|T_Q) = \prod_{n=1}^{N} \mathrm{P}(\gamma_n|T_Q) \tag{1}$$

Intuitively we sense that as the total number of views increases Γ tends toward the PDF of the target intensity echo. In the extreme case where all the views are correlated we have $\mathrm{P}(\Gamma|T_Q) \approx \mathrm{P}(\gamma_n|T_Q)$ so no ID information can be extracted from Γ.

Result 2. comes from the asymptotic behaviour of the PDF of the detection rule $\mathcal{F}(\mathbf{r}) \sim \frac{1}{N}\sum_{n=1}^{N} \mathrm{Rayleigh}^2(\sigma)$. The independence of the observations allows us to write

$$\frac{1}{N}\sum_{n=1}^{N} \mathrm{Rayleigh}^2(\sigma) \sim N.\Gamma(Nx, N, 1) \tag{2}$$

and then to deduce that:

$$\lim_{N\to+\infty} N.\Gamma(Nx, N, 1) = \delta(1-x) \tag{3}$$

Again the independence assumption allows the factorisation of the sum of the squared Rayleigh distributions. If we consider the extreme case where all the observations are dependent we would have: $\frac{1}{N}\sum_{n=1}^{N} \mathrm{Rayleigh}^2(\sigma) \sim \mathrm{Rayleigh}^2(\sigma)$ and then the speckle effect still dominates the pixel intensity behaviour.

In this paper we study the correlation between views in MIMO sonar systems using the distance correlation introduced by Székely [3]. From the distance correlation we will derive the inter-views distance correlation matrix which assess the correlation of the full MIMO system (i.e. the dependencies between each views). This independence measure matrix gives a guideline to how to build truly uncorrelated MIMO sonar systems and then maximise the performances of such system.

2. THE INDEPENDENT VIEWS PROBLEM

2.1. Definition

We define independent views as: *two views are independent if and only if their observations are statistically independent.*

2.2. The distance correlation

By introducing the term *view* we implicitly introduce the geometry and the configuration of the MIMO system. Let θ be the target view angle of the transmitter and ϕ the view angle of the receiver. The bistatic configuration of a pair of transmitter/receiver will be noted (θ, ϕ). We are interested here in knowing the level of independence of a view $V(\theta_1, \phi_1)$ with another view $V(\theta_2, \phi_2)$. To measure the dependence of 2 random variables the Pearson product-moment correlation coefficient or correlation coefficient is commonly used [4]. However the correlation coefficient suffers a number of defects: First of all this coefficient has been designed with a normal distribution assumption, this assumption does not hold in our case. Secondly this coefficient only measures linear correlation between the random variable. And finally this coefficient is not a real independence measure in the sense that the correlation coefficient of 2 random variables can be null even is these random variables are dependent. To overcome these defects we will be using the distance correlation introduced by Székely in [3]. Székely defines the distance covariance $\mathcal{V}$ as:

$$\mathcal{V}^2 = \frac{1}{c_p c_q} \int_{\mathbb{R}_{p+q}} \frac{|f_{X,Y}(t,s) - f_X(t) f_Y(s)|^2}{|t|_p^{1+p} |s|_q^{1+q}} dt ds \tag{4}$$

where f_X and $f_{X,Y}$ represent respectively the characteristic and the joined characteristic function of X or (X,Y), p and q are respectively the dimensions of the random vector X and Y, and c_d is defined as follow:

$$c_d = \frac{\pi^{(1+d)/2}}{\Gamma((1+d)/2)} \tag{5}$$

where $\Gamma(.)$ is the full gamma function. For $\mathcal{V}^2(X)\mathcal{V}^2(Y) \neq 0$ the distance correlation is then defined as:

$$\mathcal{R}^2(X,Y) = \frac{\mathcal{V}^2(X,Y)}{\sqrt{\mathcal{V}^2(X)\mathcal{V}^2(Y)}} \tag{6}$$

Székely shows in [3] that $\mathcal{R}$ has *the properties of a true dependence measure* and in particular that two random vectors X and Y are independent if and only if $\mathcal{R}(X,Y) = 0$.

2.3. MIMO inter-views dependence

To assess the inter views dependence of a MIMO system we generate randomly 10^4 targets with 2, 3, 4 or 5 scatterers. For each target we compute its response V as a function of the transmitter and receiver view angle (θ, ϕ). For each pair (θ, ϕ), $V(\theta, \phi)$ can then be considered as a random vector. The distance correlation $\mathcal{R}$ between all pairs $(\theta_n, \phi_n) \in [-\pi, \pi]^2$ is then computed. For the view angles (θ_0, ϕ_0), let $\mathcal{A}_0$ be the matrix defined by:

$$\mathcal{A}_0(\theta, \phi) = \mathcal{R}(V(\theta_0, \phi_0), V(\theta, \phi)) \tag{7}$$

Note that in the point scatterer model there is a symmetry between the transmitter and the receiver and $V(\theta, \phi) = V(\phi, \theta)$. For this reason the matrix $\mathcal{A}_0$ is symmetric along its first diagonal.

Let $\theta_1 = \theta_0 - \alpha$ and $\phi_1 = \phi_0 - \alpha$. Thanks to the axial symmetry of the problem we can write that:

$$\mathcal{A}_0(\phi, \theta) = \mathcal{A}_1(\phi - \alpha, \theta - \alpha) \tag{8}$$

So we can compute $\mathcal{A}_0(\theta, \phi)$ for only one θ_0. We then can chose $\theta_0 = 0$. For display purposes we display in Fig. 1 the distance correlation matrix $1 - \mathcal{A}_0(\theta, \phi)$ for $\phi_0 = 0$, $\phi_0 = \pi/2$ and $\phi_0 = \pi$.

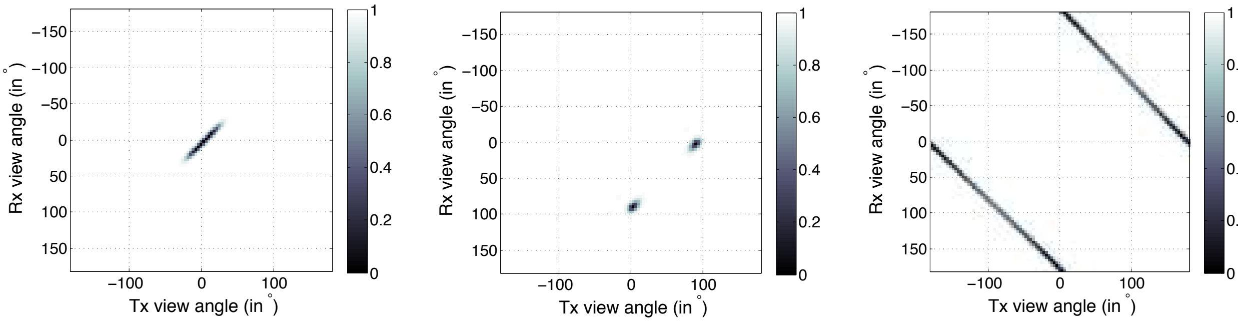

(a) (b) (c)

Fig. 1: Distance correlation matrix $1 - \mathcal{A}_0(\theta, \phi)$ for (a): $\phi_0 = 0$, (b): $\phi_0 = \pi/2$ and (c): $\phi_0 = \pi$.

Fig. 1(a) displays the monostatic case, the transmitter and the receiver are in the same position: $\theta_0 = \phi_0 = 0$. Even though the monostatic configuration is convenient from a practical point of view it does not offer the best view in term of correlation. The monostatic view correlates strongly with its neighbours $(\theta = +\alpha, \phi = -\alpha)$ for $\alpha \in [-25°, +25°]$. It is interesting to note that the monostatic view correlates as well with $(\theta = \alpha, \phi = \alpha)$ for $\alpha \in [-6°, +6°]$. So if we consider a monostatic sonar turning around the target for a full 360°, an average around 30 independent views will be obtained which is insufficient to achieve super-resolution. In Fig. 1(c) the target is in-between the transmitter and the receiver. Although this configuration is not practical as the transmitted wave will arrive at the same time as the target echo to the receiver, it is interesting to note that all the opposite views $(\theta, \theta + \pi)$ for all θ correlate strongly. In Fig. 1(b) displays the distance correlation matrix with $\phi_0 = \pi/2$. As predicted we observe a symmetry along the first diagonal and $\mathcal{A}_0(\theta, \phi) = \mathcal{A}_0(\phi, \theta)$. The correlation peaks are focussed on (θ_0, ϕ_0) and (ϕ_0, θ_0). This configuration is the must effective as far as its independence is concerned. And the independence of this view toward its neighbours is maximised.

2.4. MIMO geometry and super-resolution

In the following simulation we aim to demonstrate that we can recover the geometry of a target (*i.e.* the location of its scatterers). Given the results presented in Fig. 1 we chose a "L" shape MIMO configuration as pictured in Fig. 2. The transmitters are placed in the x-axis, the receivers are on the y-axis. For this experiment we place the transducers an equal spacing along the axis. The number of transmitters and receivers and the spacing between them is adjustable. The MIMO system will use the frequency band 50 kHz to 150 kHz. We consider a 3 point scatterers target, the scatterers are separated by one wavelength. Note that we are considering the central frequency of the MIMO system (100 kHz). Under this condition one wavelength corresponds to 1.5 cm.

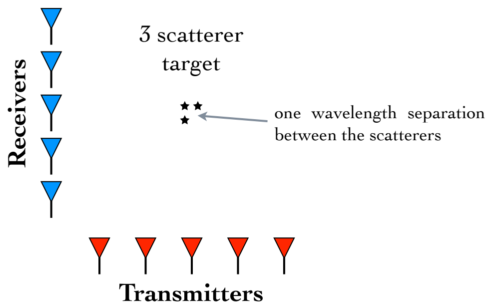

Fig. 2: MIMO configuration.

In order to image the output of the MIMO system we will use the multi-static back-projection algorithm which is a variant of the bistatic back-projection algorithm developed by the Synthetic Aperture Radar (SAR) community. Further details can be found in [5–7]. Using the back-projection algorithm the Synthetic Aperture Sonar (SAS) image is computed by integrating the echo signal along a parabola. In the bistatic case the integration is done along ellipses. For the multi-static scenario the continuous integration is replaced by a finite sum in which each term corresponds to one transmitter/receiver pair contribution.

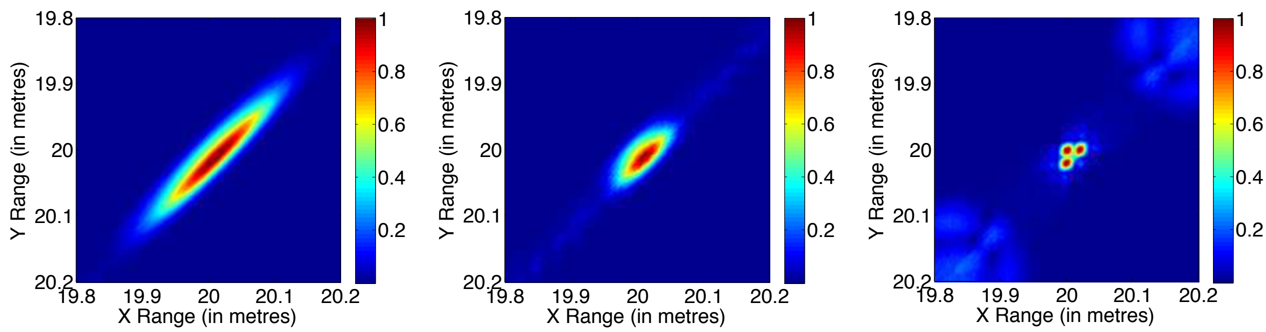

Fig. 3: 3 scatterers target MIMO image using: (a) 10 transmitters and 10 receivers with 20 cm spacing, (b) 3 transmitters and 3 receivers with 3 metres spacing and (c) 10 transmitters and 10 receivers with 3 metres spacing.

In Fig. 3(a) we have considered a MIMO system with 10 transmitters and 10 receivers with a spacing of 20 cm. For this scenario the 20 cm spacing breaks the widely spaced antenna assumption and the views are not exactly independent between each other. For this reason we only observe a blob of energy at the target location. In Fig. 3(b) the MIMO system consists in 3 transmitters and 3 receivers with 3 metres spacing. In this case the spacing between the antennas is several hundreds of wavelengths so the independence of the views is respected. The total number of views however is 3 × 3 = 9 independent views which is relatively low according to the convergence speed of Eq. (3). In this scenario the number of views is too low to ensure the decorrelation of the scatterers within the target. For this reason only a blob of energy marks the target location. However by closely inspecting to the central blob it is possible to distinguish a structure. Finally in Fig. 3(c) we consider a MIMO system with 10 transmitters and 10 receivers with a spacing of 3 metres. With this configuration we respect the conditions stipulated earlier and we are able to clearly image the 3 scatterer target in so doing achieve super resolution imaging.

2.5. Inter-correlation for full MIMO systems

It is interesting to compare these results to the intra-views correlation of the different MIMO systems. Let note $\{(\theta_n, \phi_n)_{n\in[1,N]}\}$ the views of the MIMO system. The level of inter-correlation for the full MIMO can be computed as:

$$\mathcal{B}(\theta,\phi) = \max_{n\in[1,N]} \mathcal{A}_n(\theta,\phi) \tag{9}$$

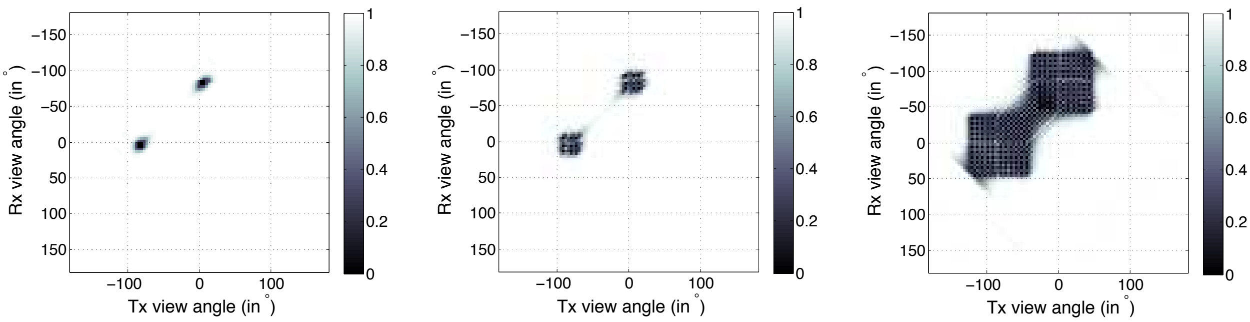

(a) (b) (c)

Fig. 4: Full MIMO inter-correlation distance matrix $1-\mathcal{B}(\theta,\phi)$ *for (a) 10 × 10 with 20 cm separation, (b) 3 × 3 with 3 m separation and (c) 10 × 10 with 3 m separation.*

In Fig. 4 we plot the $1-\mathcal{B}(\theta,\phi)$ functions for the same MIMO configurations as the ones explained in Fig. 3. In Fig. 4(a) we are considering the 10 × 10 MIMO system with 20 cm separation between antennas. The 100 views produced by this configuration are all concentrated around the (0°,-90°) view and are clearly all correlated to each other. The independent views assumption breaks down. In Fig. 4(b) the 3 × 3 MIMO configuration is considered. The 3 m spacing between the antenna ensures the independence of the views and we can clearly see in the cluster 9 peaks corresponding to each view. In Fig. 4(c) the 10 × 10 MIMO configuration is considered. Again the 3 m antenna separation provide the necessary independence between the views and the 100 correlation peaks are visible and distinct between each other. The $\mathcal{B}(\theta,\phi)$ inter-correlation distance matrix then gives us an insight on how to design an efficient MIMO system and ensure the views independence. Assuming that the MIMO system provides enough views for recognition or super-resolution, each views (θ_n, ϕ_n) in the $\mathcal{B}(\theta, \phi)$ should decorrelate as much as possible with the other views $(\theta_m, \phi_m)_{m \neq n}$

For comparison purposes we have computed the SAS image of the same target as described in Fig. 2 using the same frequency band and at the same range than the previous experiment. The SAS image of the target is displayed in Fig. 5.

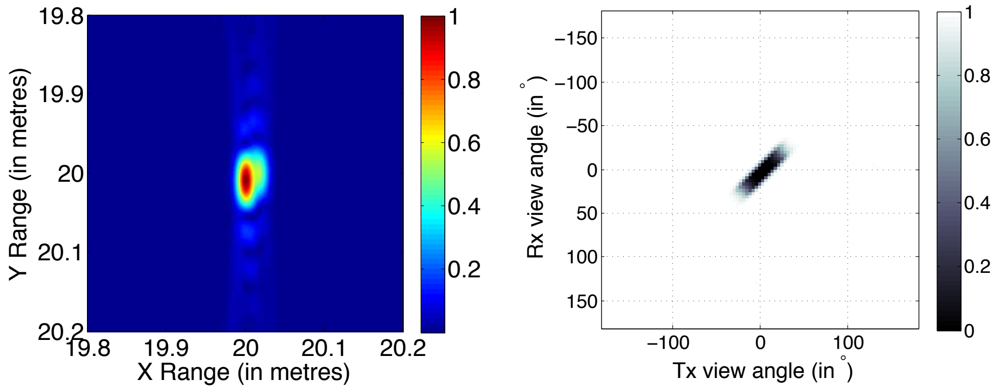

(a) (b)

Fig. 5: 3 scatterers target using SAS system. (a) SAS image, (b) $1 - \mathcal{B}(\theta, \phi)$ *function for the SAS configuration.*

The SAS system run at 20m range from the target in a straight line. The beamwidth is fixed to 10°. We compute the target echo at every $\lambda/2$. In total 467 echoes are computed and the SAS image is formed using back-propagation algorithm. Despite the high number of views and because all the SAS subviews are highly correlated between each other as shown in Fig. 5(b), the SAS system fails to separate the 3 scatterers. Earlier we saw that monostatic systems correlate in average for 12°. A 10° beamwidth SAS system then sees at the maximum 2 to 3 independent views of a target. Note that on this aspect the SAS image reconstruction is based on the hypothesis that each pixel contains one scatterer point. And then SAS systems requires strong correlation between consecutive views in order to track and correct the echoes phase changes. So in that aspect it is not surprising that the mono-views from SAS systems are so strongly correlated to each other.

3. CONCLUSION

In this paper we were able to relate independent observations to independent views for MIMO systems. We derived the MIMO inter-views dependence and then the full MIMO system inter-correlation factor using the distance correlation introduced by Székely. We showed that the 90° bistatic view is the one which correlates the less to the other views and the one which is the more compact in the MIMO inter-correlation distance plane. With those results a fully independent inter-views MIMO system was designed and we demonstrated that such system has the predicted MIMO capability especially such system can archive super resolution.

4. ACKNOWLEDGEMENT

This work was supported by the Engineering and Physical Sciences Research Council (EPSRC) Grant number EP/J015180/1 and the MOD University Defence Research Collaboration in Signal Processing.

REFERENCES

[1] Y. Pailhas, Y. Petillot, C. Capus, and K. Brown. Broadband mimo sonar system: a theoretical and experimental approach. In *3rd International Conference and Exhibition on Underwater Acoustic Measurements: Technologies & Results, Nafplion, Greece*, 2009.

[2] Y. Pailhas, Y. Petillot, C. Capus, and B. Mulgrew. Target detection using statistical mimo. In *European Conference on Underwater Acoustics, ECUA12*, 2012.

[3] G. J. Székely, M. L. Rizzo, and N. K. Bakirov. Measuring and testing dependence by correlation of distances. *The Annals of Statistics*, 35:2769–2794, 2007.

[4] J. L. Rodgers and W. A. Nicewander. Thirteen ways to look at the correlation coefficient. *The American Statistician*, 42(1):5966, 1988.

[5] N.J.Willis. *Bistatic Radar*. Norwood, MA:ArtechHouse, 1991.

[6] A. Home and G. Yates. Bistatic synthetic aperture radar. *IEEE RADAR 2002*, pages 6–10, 2002.

[7] O. Arikan. A tomographic formulation of bistatic synthetic aperture radar. In *Procedings of ComCon 88*, 1988.